Combining induction control and wake steering for wind farm energy and fatigue loads optimisation

IOP Conf. Series: Journal of Physics: Conf. Series **1037** (2018) 032011 doi:10.1088/1742-6596/1037/3/032011

Combining induction control and wake steering for wind farm energy and fatigue loads optimisation

Ervin Bossanyi

DNV GL, One Linear Park, Avon Street, Bristol, BS2 0PS, UK

ervin.bossanyi@dnvgl.com

Abstract. Turbine power and yaw set points can be adjusted across a wind farm to minimise the overall power losses and the additional fatigue loads caused by wake interactions. Detailed modelling is required to understand the complex flows in sufficient detail to allow a realistic practical control design. High-fidelity computational fluid dynamics requires enormous computational resources, so simpler engineering models are needed which capture the most important effects while running fast enough to allow sufficient testing. This paper describes a steady-state optimisation tool which has been extended to optimise all the power reduction set-points and yaw offsets simultaneously for different wind conditions. It also describes a fast time-domain simulation model which captures turbine and wake dynamic effects, so that wind farm controllers of all kinds can be tested in realistic and time-varying conditions. To demonstrate its application for controller testing, the performance of the combined power and yaw controller is tested during changing conditions of wind speed, direction and turbulence derived from measured site data. Finally, the need for validation is discussed, as many uncertainties still need to be resolved in order to obtain sufficient confidence that the potential benefits of such wind farm control schemes can be realised in practice.

1. Introduction

There is currently a great deal of interest in the possibility of reducing wake interaction effects in a wind farm by manipulating the turbine control actions in order to weaken the wakes (induction control) or to steer them away from downstream turbines by introducing yaw misalignments (wake steering control). Changing a turbine's wake properties implies moving away from the design control settings which are presumably designed for optimal performance of the turbine when operating in isolation. Therefore, any form of wake manipulation involves a trade-off between reduced performance of the manipulated turbines and improved performance at other turbines such that the overall wind farm performance is improved. In this context, performance could mean energy production, fatigue loading, or both, so the aim would be to increase total wind farm energy production and/or to reduce or even out the accumulation of fatigue damage across all the turbines.

While the principles of this kind of wind farm wake control have been discussed for at least 25 years, e.g. [1], successful practical applications have yet to be demonstrated convincingly. Simulation models suitable for designing and testing wind farm controls are being developed, but it is not easy to reach a good compromise between fidelity and speed, due to the wide range of physical effects which have to be taken into account: turbulent atmospheric boundary layer flows which vary greatly according to atmospheric stability, turbine wakes which interact in subtle ways with the boundary layer and with each other, and the performance and loading of the turbines themselves when operating

in the resulting non-homogenous flow. The models being used vary widely [2], ranging from high-fidelity computational fluid dynamics (CFD) models such as large eddy simulations (LES), which should be able to capture most of the relevant effects but require enormous computing resources to run, through Reynolds-averaged Navier-Stokes (RANS) models, to simple empirical models fitted to experimental data. This paper presents an engineering model capable of dynamic time-domain simulation of a wind farm, including a correlated turbulent wind field which can vary with changing wind conditions over a long period of time, dynamic wake effects such as meandering, and turbine dynamics and control actions which can be modified by a wind farm controller.

Whether using induction control or wake steering, methods for designing and implementing suitable wind farm controllers range from quasi-static open-loop control or 'advanced sector management', which may work quite satisfactorily as long as wind conditions are slowly-varying, to dynamic closed-loop control schemes which may offer faster response and greater tolerance to imperfect modelling assumptions by making use of detailed real-time measurements across the whole wind farm to infer the behavior of the individual wakes.

This paper demonstrates the possibility of combining both induction control and wake steering into an optimized Advanced Sector Management scheme, using pre-calculated look-up tables of turbine power and yaw set-points as a function of the meteorological conditions averaged across the site, such as may be obtained from filtered met mast measurements or aggregated turbine SCADA data. Set-points are optimised iteratively using a very fast steady-state wake model, and the performance of the resulting controller in dynamic conditions, with wind conditions changing over a period of time, is demonstrated using the time-domain simulation model. In a previous paper [1], this process was used to design and test a wind farm controller using induction control only, using a generic 2MW turbine model. In this paper, using the same turbine model, the use of wake steering in combination with induction control is shown to provide additional benefits.

Although some interesting results are obtained, there are still significant uncertainties to be tackled before such technology can be considered commercially mature, with a need for detailed field tests to validate the models over a wide range of conditions, and to confirm the benefits that may be achievable in practice through the wind farm control action.

2. Tool chain

The work in this paper has been carried out using a set of software tools obtained by interfacing and extending a number of DNV GL's existing commercial tools, as illustrated in Figure 1.

The key new elements are the set-point optimizer and the dynamic wind farm simulator, described below, and some example results are presented in Section 3. The set-point optimiser uses the fast steady-state wake model of WindFarmer [4] iteratively to optimise the wind farm performance against a cost function involving energy production and turbine fatigue loads [6]. Set-points are generated for a whole range of wind speeds, directions and turbulence intensities. The resulting wind farm controller is then tested using the dynamic wind farm simulator. This was demonstrated in [3] for induction control only. In Section 3, this paper demonstrates the extension of the set-point optimiser to generate optimal power delta and yaw set-points simultaneously, and the use of the dynamic wind farm simulator to test the resulting controller. The remainder of Section 2 describes the tools in more detail.

2.1. Fatigue loads database

Several thousand single-turbine 10-minute turbulent simulations with full turbine and controller dynamics, covering a full range of wind speeds, turbulence intensities, delta set-points and yaw misalignments, were run in a few hours using the cloud computing facility of *Bladed*, and the results processed into a database of power, thrust coefficients and fatigue loads.

2.2. Steady-state set-point optimiser

To allow for wake steering control, the WindFarmer [4] wake model was extended to allow yaw misalignments and provide the resulting lateral wake deflection, for which the model of Jiménez [7]

has been used. Delta control, which reduces power output by a given amount at any wind speed by increasing blade pitch, is already included as in [6]. Delta and yaw set-points for all the turbines are combined into one set-point vector, and a simulated annealing algorithm is used to optimise this vector against the chosen cost function, which is evaluated at each step by interpolation from the fatigue loads database. The same database also provides the thrust coefficients used by the wake model.

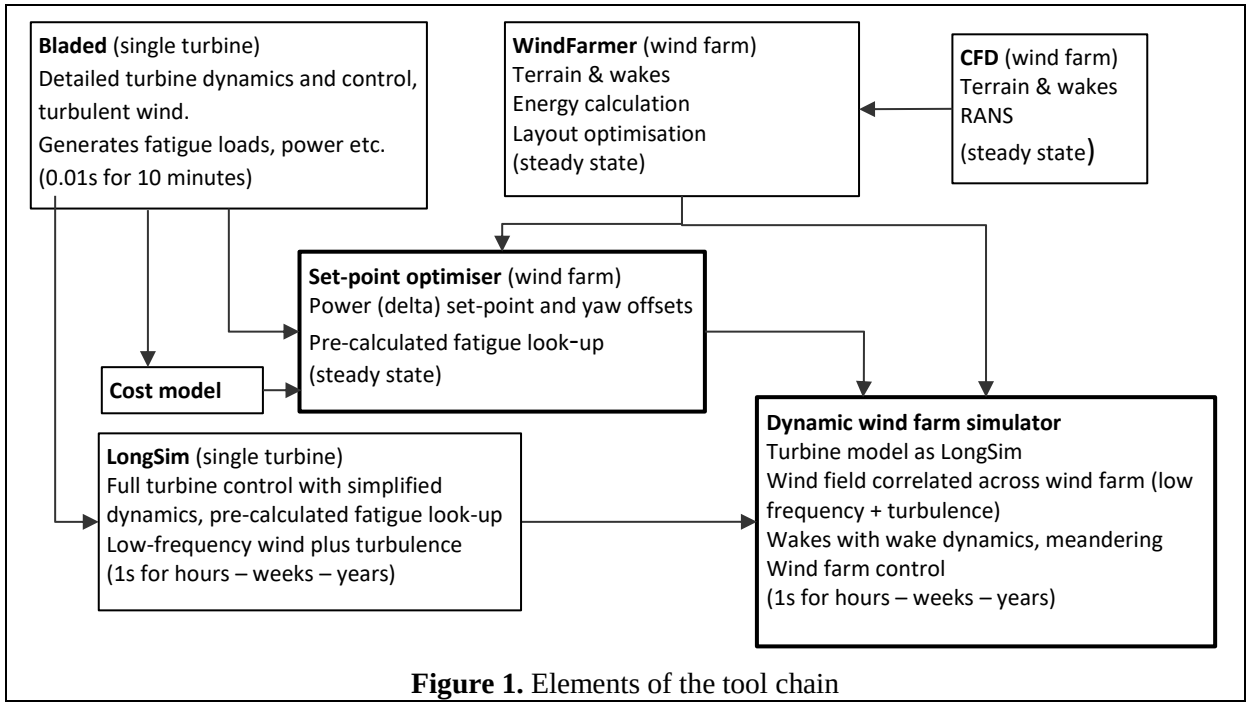

Figure 1. Elements of the tool chain

2.3. Dynamic wind farm simulator

The dynamic wind farm simulator runs with a short enough time step to represent the turbine rotor speed and pitch degrees of freedom and the turbine control action (including yaw control), driven by synthetic high-frequency turbulence. Lower-frequency turbulence generated to follow measured site data, e.g. from a met mast over a period of time, is spatially correlated across the wind farm and drives wake advection and meandering. The procedure allows simulations to track changing wind conditions over long periods: hours, days or even years, while also modelling the turbine and control dynamics with time steps down to 1s or less. The model extends an existing single-turbine model [20] to a whole wind farm, in a way that has some conceptual similarities to SimWindFarm [21] and the model of Poushpas [22], for example. Further details of the model are provided in the next paragraphs.

2.3.1. Turbine aerodynamics. 2D look-up tables of power and thrust coefficients are generated from Bladed, as a function of tip speed ratio λ and pitch angle β. The effect of yaw misalignment is also needed, firstly to predict power production accurately given the inevitable yaw misalignment variations which occur in practice and in the model, and secondly to model deliberate yaw misalignments due to wake steering control. Using a set of *Bladed* runs with steady wind conditions, an empirical fit for the effect of yaw misalignment γ on the power coefficient was derived for the generic 2MW turbine, of the form $C_P(\lambda,\beta,\gamma) \approx C_P(\lambda,\beta).(\cos\gamma)^{f(\beta)}$. The polynomial expression $f(\beta) = a + b\beta + c\beta^2$ was found to give a reasonable fit, with $a = 1.476$, $b = 3.2715$ and $c = 15.783$. Default aerodynamic settings in *Bladed* v4.8 were used, including the Glauert skewed wake correction. The yawed C_P is defined using horizontal wind speed magnitude V and nominal rotor swept area, i.e. Power / $(\frac{1}{2}\pi R^2 \rho V^3)$.

2.3.2. Turbine dynamics. A simple dynamic model is used, consistent with using a timestep in the region of 1 second, so higher-frequency structural dynamics are not represented. The rotor speed and blade pitch degrees of freedom are implemented, together with nacelle yaw. The first tower fore-aft mode could be readily implemented if desired. Sensor and actuator responses are modelled, including the speed sensor time constant, generator torque actuation time constant, pitch actuation time constant and/or second-order response, and yawing at a constant rate.

2.3.3. Turbine control – power production. Standard PI(D)-based torque and collective pitch control are implemented, with pitch gain scheduling. Below-rated C_P-tracking uses either a standard quadratic gain or a look-up table. Transitions at rated wind speed between torque and pitch control use bias terms. All these features are defined in [8]. The bias terms are calculated from an estimated wind speed, for which a Luenberger observer is available, but an ideal estimator using the rotor-average wind speed is usually allowable given the time step used.

Delta control is implemented as described in [9]. The estimated wind speed drives a parallel representation of the turbine and controller dynamics without delta control (and without yaw misalignment) to define the maximum power available at any instant. The power delta is subtracted from this, and the torque demand to the power converter is reduced by the amount necessary to achieve this reduced power. At the same time, the fine pitch is increased to maintain the desired rotor speed. The net result is that the power reduction is achieved by increasing the pitch angle while keeping the same rotor speed.

2.3.4. Turbine control - supervisory. Supervisory control (including yaw control) is flexibly implemented. A syntax is provided so that the user can define typical filters and alarms. Filters are typically low-pass filters for generator speed, yaw misalignment (wind vane signal), wind speed (nacelle anemometer) etc. Alarms can respond to filter outputs using conditions which can include thresholds and durations (time since threshold crossing), latches, etc. Nacelle anemometry corrections for rotor influence are assumed to be included in the calibrations.

For the particular simulations in Section 3, a standard yaw controller is used with an averaging time constant of 30 seconds and a dead-band of 8º. The yaw rate is fixed at 0.3º/s,

2.3.5. Turbine loads. To run fast, the turbine model does not include structural dynamics nor spatial variations in turbulence across the rotor, and cannot therefore generate fatigue loads directly. The loads are therefore interpolated from the Fatigue Loads Database (FLD – section **Error! Reference source not found.**) in a post-processing step. This is a pragmatic approach with some deficiencies, e.g. wake turbulence does not have the same characteristics as ambient turbulence just with an increase in turbulence intensity; and low-frequency variations such as wake meandering will also affect the fatigue loading to some extent. To help understand whether this is important, the FLD Bladed runs will be extended in future to include the specific effects of upwind turbine wakes, including meandering, at a cost of a further increase in the database size.

2.3.6. Wind field. To minimise computation requirements, the wind field is divided into low-and high-frequency parts separated by a user-specified cut-off wavelength, typically corresponding to a spatial resolution of around two turbine diameters ($\Delta x = 2D$). Lower-frequency variations are correlated across the wind farm using coherence functions, and cause wake meandering and advection. Higher-frequency variations, uncorrelated between turbines, are then superimposed at each turbine, along with the wake velocity deficits of any upstream turbines, and with the local turbulence intensity increased according to the wake turbulence model (Section 2.3.8).

The wind field generation starts from single-point measured data, e.g. 10-minute averages of wind speed, direction and standard deviation from a met mast. A smooth time history is fitted which preserves the correct 10-minute averages, and synthetic turbulence is then added, using an assumed turbulence spectrum (e.g. Kaimal). The spectrum is divided at the cut-off wavelength corresponding to

Δx. Since the low-frequency variations must cover the entire range of wind speeds and directions, the spectrum and coherence functions are expressed in terms of wavenumber rather than frequency, as they then become largely independent of wind speed. The Veers method [10] is used to generate correlated low-wavenumber histories at a grid of points covering the wind farm area at hub height. To simulate advection, the phases at wavenumber k are adjusted by $2\pi kx$ at downwind distance x prior to the inverse FFT step. While the wind field includes all three components of turbulence, the lateral (and vertical) are zero-mean, so gross changes in wind direction are added from the smoothed mast data. For rapid direction changes an assumption is needed about how the direction change propagates through the farm: e.g. at the mean speed, and the local wind vectors are rotated accordingly.

For the coherence, the mesoscale model from Larsen [11] is merged with the IEC models [12] for turbulent fluctuations (the Kaimal version has been used here). An exponential decay model is used for alongwind coherence in the turbulent range, but there is significant variation in the literature over the decay constant to use, and so more experimental data on this would be useful. For the simulations below, decay constant β=1 was used, where squared-coherence is defined by $\exp(-\beta kd)$ for alongwind distance d and wavenumber k defined as frequency (Hz) divided by wind speed.

High frequency turbulence is generated using inverse FFT of the relevant part of the spectrum to give the hub wind speed, and again with a low-pass filter applied to give rotor-average wind speed.

2.3.7. Wake profile. The Ainslie model [13] is used by default, based on an axisymmetric eddy-viscosity solution of the Navier-Stokes equation. It produces a Gaussian-shaped velocity deficit profile as from 2 diameters downstream, becoming wider and shallower further downstream, depending on turbulence intensity, while conserving momentum in the flow. The formulation used in WindFarmer [4] is used, having been validated against many wind farm measurements [5] at least in terms of 10-minute mean power production.

2.3.8. Wake turbulence. As in WindFarmer [4], wake turbulence is currently modelled using the completely empirical Quarton-Ainslie model ([14] as modified in [15]), although a more theoretically-based model would be desirable.

2.3.9. Wake meandering. The dynamic wake meandering model of Larsen *et al* [16] assumes that the wake is pushed around laterally and vertically by the low frequencies of the turbulence, defined as spatial scales greater than two 'wake diameters'. Here the low-frequency wind field (Section 2.3.6) is used to drive the meandering; a fixed cut-off wavelength is needed, so two turbine diameters has been used. The parameterisation of the Ainslie wake deficit model has been calibrated against 10-minute average wind farm measurements where wake meandering would have caused the mean wake deficit profile to be 'smeared out' laterally and vertically. Ainslie [13] suggested a way to calculate this broadening effect. For the dynamic simulation, an instantaneous wake profile before meandering is needed. This is obtained by applying the inverse of the Ainslie correction to the mean profile. Simulation results averaged over time confirm that the meandering then causes the a 'smeared out' profile which matches the 10-minute average behaviour, as shown in Figure 2.

2.3.10. Wake advection. Any change to the wake profile caused by turbine control action or changing wind conditions must advect downstream. Just like lateral and vertical wake meandering, this advection is assumed to be driven by the longitudinal component of the low-frequency wind field. However, the reduced wind speed in the wake itself probably causes the wake advection speed to be lower than the free wind speed. There is little information in the literature to quantify this effect; in [17] some results are reviewed, suggesting that the advection speed may be around 80% of the free wind speed, but that it also depends on turbulence and downstream distance. Different options are therefore provided in the model; for the simulations reported here, an average of the free wind speed and the mean wake speed over the profile was used.

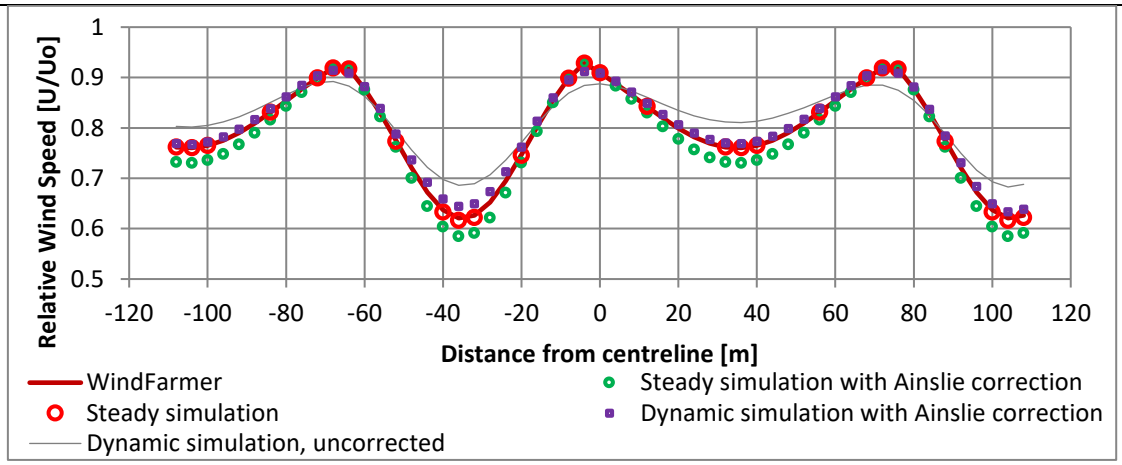

Figure 2. Wake deficit profile behind four turbines at different distances. Red: model calibrated for 10-minute average data. Green: inverse Ainslie correction gives narrower, deeper wakes. Purple: dynamic meandering then restores the correct mean profiles.

2.3.11. Wake deflection. For a turbine with yaw misalignment, the wake will be deflected laterally. Jiménez [7] derives a simple model for this effect, based on momentum conservation with a rectangular wake deficit profile, but the same model has been used for other wake profiles, e.g. in Gebraad [18], where the deflection recovery parameter has been tuned against CFD simulations; this model has been used in the simulations below, but more sophisticated models are also available.

2.3.12. Wake superposition. The combined effect of two or more wakes on a downstream turbine is not well understood, and different models have been proposed in the literature. By default, the 'dominant wake' model used by WindFarmer [4] is used, where only the highest velocity deficit and the highest added turbulence of all the wakes impinging on a turbine are used. According to CFD calculations in [19], this works well for aligned turbines, while a linear combination of wake deficits may work better in cases where the wake centrelines are offset. Further work using CFD or wind tunnel results should help to define a more generalised model.

2.3.13. Wind farm control. The wind farm control module is flexibly implemented to allow any different controllers to be tested. It has access to model information such as would be expected to be available to a wind farm SCADA system, and outputs power delta and yaw set-points to all the turbines. The wind farm controller used in this paper is defined in Section 3.2.

3. Example results

Here the tool chain is used to illustrate the process of designing a wind farm control algorithm and testing it in dynamic simulation during changing wind conditions. The example uses a very simple wind farm consisting of a row of six generic 2MW wind turbines spaced 5 diameters apart in a straight line at 91º from the North-South direction.

3.1. Steady-state optimisation

First the steady-state optimiser was used to generate optimal delta and yaw set-points for 45 different wind conditions: 3 turbulence intensities (4%, 7%, 10%) by 3 wind speeds (9, 10, 11 m/s) by 5 directions (86º to 94º in 2º steps). Two illustrative cost functions were used: "Energy Only" (100% weighting on energy production), and "Energy & Loads" (relative decreases in tower base and blade root bending moments each given 10% weighting compared to increases in energy production). The optimiser was run for a set time at each wind condition, since it is not possible to ascertain proximity to the true global optimum. An example result for one wind condition is shown in Figure 3: optimising

on "Energy & Loads" for 1800s gave the set-points shown at top right, resulting in increased power production and reduced loads compared to the base case. (The 'Ideal' case is without wake effects.)

3.2. Wind farm controller

For the simulations in this paper, look-up tables define the delta and yaw set-points as a function of farm wind speed, direction and turbulence intensity, for which the smoothed met mast measurements are used, further filtered using a 30s time constant. The control action is updated every 5s.

Initially the yaw set-points were sent to the turbines simply as offsets to apply to the turbine's yaw controller, but the dead-band hysteresis resulted in slow response, so it was better for the wind farm controller to send a demanded nacelle direction, and make the turbine respond to this more directly (at the normal yaw rate) with just a small dead-band (here 5º) on integrated yaw position error (although the individual turbine yaw control could still act in case of large local deviations).

It is important to note that changes to the detail of the yaw control strategies can change the energy production by amounts comparable to the changes brought about by the wind farm control itself. It is therefore important to ensure that the yaw control strategy used in the base case and the strategy used with wind farm control are both realistic and well optimised, to ensure that the benefit of wind farm control is fairly assessed. As it happens, the optimisation of these strategies is actually one of the tasks for which the dynamic simulator was first developed [20], allowing energy production to be traded against numbers of yaw manoeuvres for example, given site-specific long-term wind variations. For the results in this paper, the strategies are not fully optimised, but a few variations were tried in each case to achieve results which appear reasonable.

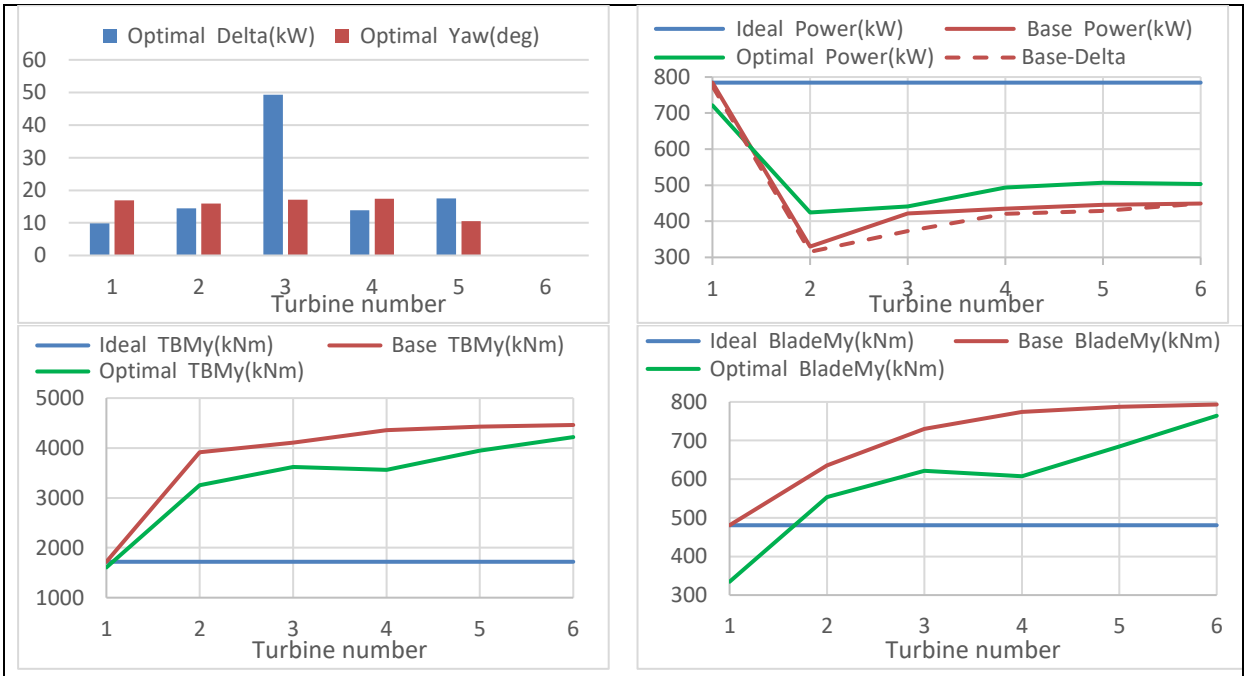

Figure 3. Example steady-state optimisation for 9 m/s, 4% turbulence, wind direction 4º from row.

3.3. Dynamic simulation

To test whether these set-points could be usable in practice to achieve the desired improvement in wind farm performance, the dynamic wind farm simulator was used to run a 3-hour example simulation. A 3-hour period of measured data from the FINO-1 met mast in the German North Sea was selected as input, with changing wind conditions (wind speed, turbulence intensity and wind direction) as shown in Figure 4. This dataset was used to generate a correlated wind field for the wind

farm, and the same met mast measurements were also used as the inputs to the wind farm controller. The controller applied a low-pass filter to each signal before calculating delta and yaw set-points for each turbine by linear interpolation from the 45 sets of quasi-static set-points.

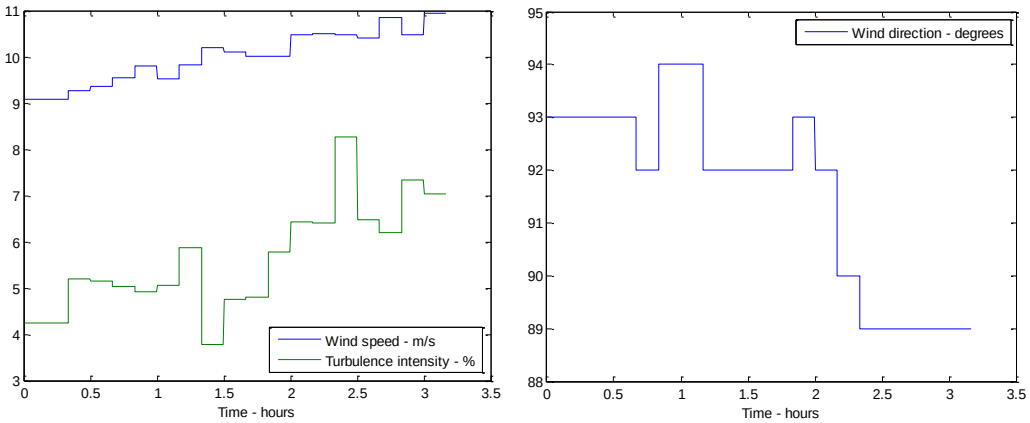

Figure 4. Wind conditions for simulation (measured at FINO-1 mast)

Using set-points generated for "Energy & Loads" optimised for1800s, the resulting set-point time histories for all the turbines are shown in Figure 5. The total wind farm power, tower base moment and blade root moment are shown in Figure 6. Figure 7 shows the total energy and loads benefit when the same 3-hour simulation was repeated with set-points from different runs of the set-point optimiser. For the case shown in Figure 5 and Figure 6, the energy increase was 2.06%, with loads reduced by 2.86% and 4.16% at the blades and tower respectively. Set-points obtained after short optimisation times produced much greater load reductions, but an energy increase is harder to find, requiring longer optimisations. "Energy & Loads" optimisation seems to give almost as much energy increase as "Energy Only", and the loads decrease in both cases, suggesting that a simple "Energy Only" optimisation may be a reasonable one to use; but "Energy & Loads" delivers much greater load reduction with very little compromise on energy.

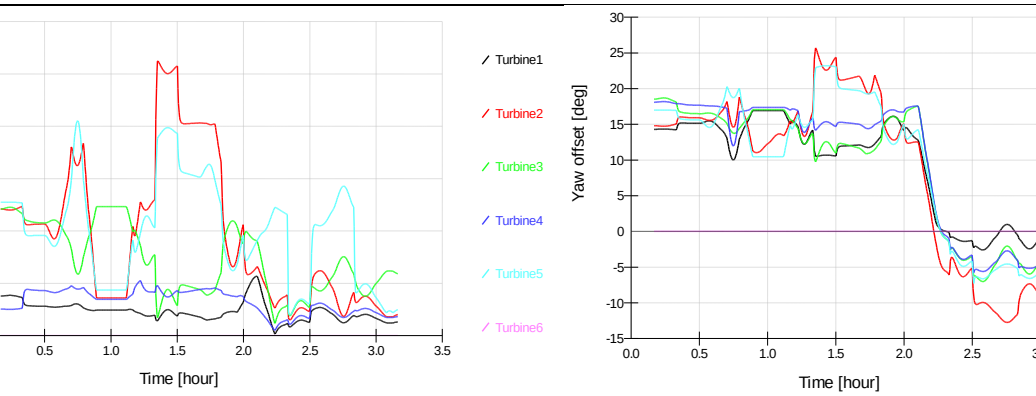

Figure 5. Example time histories of delta set-points (left) and yaw offsets (right) for all the turbines

4. Further developments

Many further improvements to the simulation model are planned, such as enhanced modelling of wake deflection, wake superposition, effect of wind shear, etc. These are planned in parallel with validation by comparison against CFD models, wind tunnel tests and field measurements.

Of course, many variations on the wind farm control algorithm can also be tested with the model. For example, rather than using met mast data for the wind inputs to the advanced sector management

algorithm, SCADA data from unwaked turbines can be used (with a simple direction-based algorithm to determine which turbines are unwaked). Speed and turbulence estimators in the turbine controllers would be useful for this. Such inputs may need less filtering to be representative of the whole wind farm, and of course there may not always be a met mast anyway. Filter time constants, yaw algorithms and the controller update interval can also be optimised using the model.

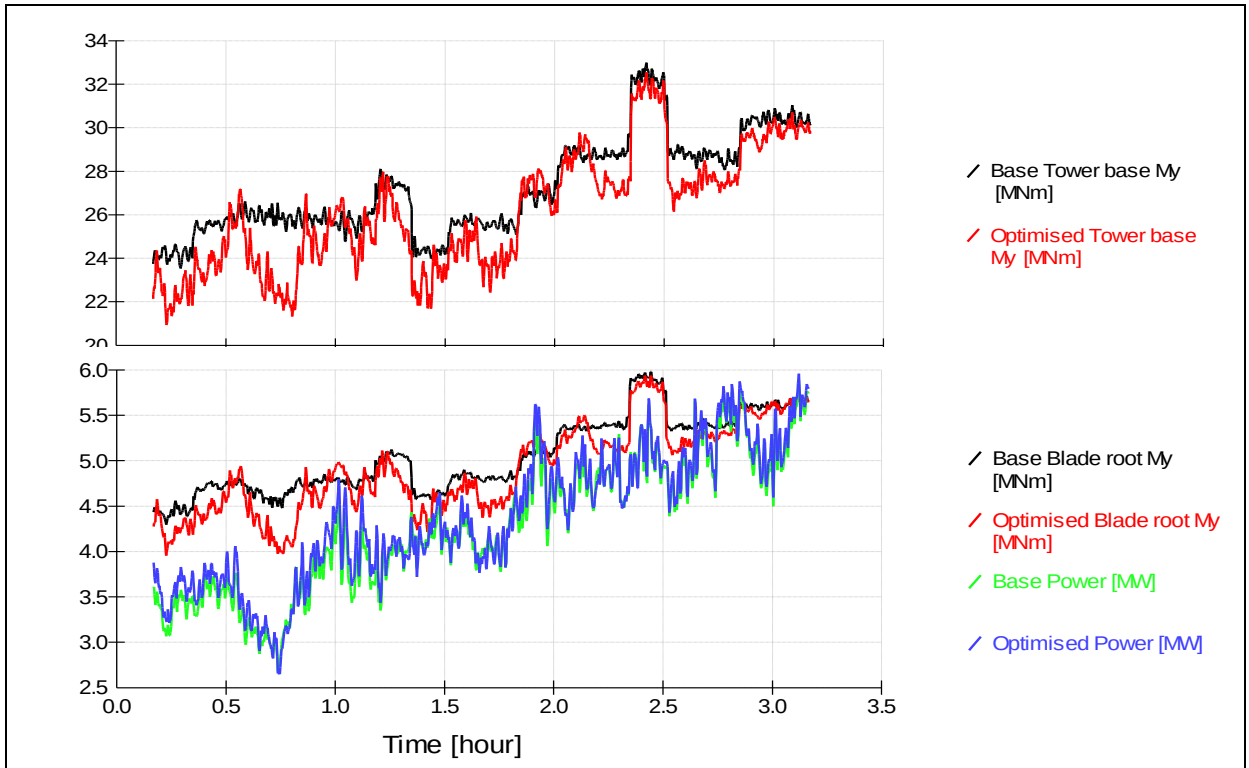

Figure 6. Total wind farm power and loads: Base case and optimised (1800s, Energy & Loads)

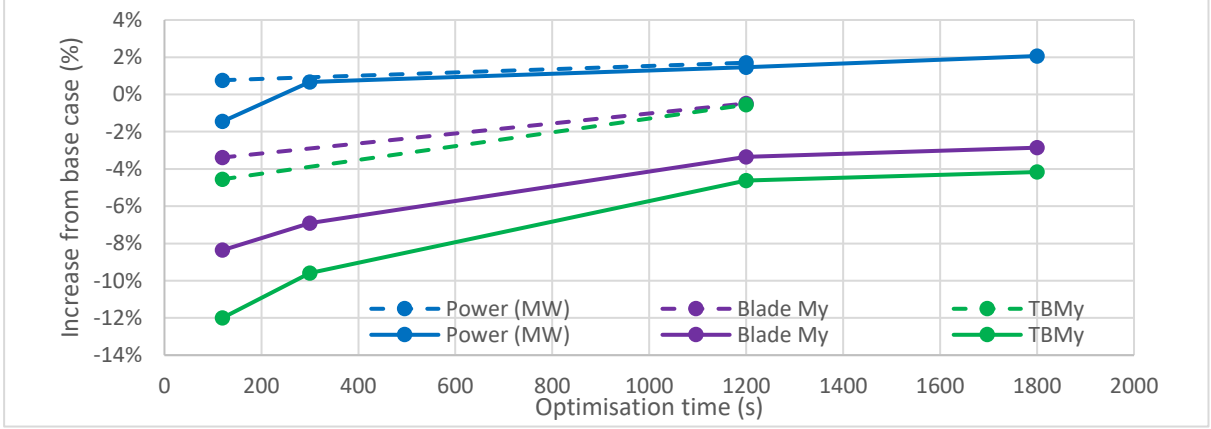

Figure 7. Benefits obtained during 3-hour dynamic simulation, as a function of the time for which the steady-state optimiser was allowed to run. Dashed lines: optimised on energy only, Solid lines: optimised on energy and loads.

5. Conclusions

A tool chain suitable for wind farm controller design and simulation testing has been presented. Using induction control and wake steering in combination, increased energy capture together with reduced fatigue loading should be achievable. The benefits depend critically on the accuracy of the wake

models, but uncertainties are still quite high, especially for aspects such as wake mixing and effects of atmospheric stability, so initial deployment is envisaged as a confidence-building process in which model enhancements and refined control techniques continue to be developed hand in hand with feedback and validation from measurements on real wind farms. Suitable measurement campaigns are far from straightforward, but a number of such campaigns are already being planned in the wind energy community, and are essential for mitigating the many remaining uncertainties and to provide confidence that the potential benefits of such wind farm control schemes can be realised in practice in a commercial context.

References

[1] Spruce C 1993 Simulation and Control of Windfarms, *PhD Thesis* (University of Oxford).
[2] Sanderse B 2009 Aerodynamics of wind turbine wakes, ECN-E--09-016 (ECN).
[3] Bossanyi E 2017 Dynamic wind power plant simulator for wind farm controller testing *Proc. Wind Energy Science conference* (Copenhagen: European Academy of Wind Energy).
[4] DNV GL 2014 *WindFarmer Theory Manual v5.3*
[5] DNV GL 2014 *WindFarmer Validation Report* (Bristol: Garrad Hassan & Partners Ltd.).
[6] Bossanyi E and Jorge T 2016 Optimisation of wind plant sector management for energy and loads *Proc. 2016 European Control Conference* (Aalborg: European Control Association).
[7] Jiménez A, Crespo A and Migoya E 2010 Application of a LES technique to characterize the wake deflection of a wind turbine in yaw *Wind Energy*, **13**-6:559–572, 2010.
[8] Burton T *et al* 2011 *Wind energy handbook* Second edition, John Wiley & Sons Ltd.
[9] Bossanyi E 2015 Generic grid frequency response capability for wind power plant *Proc. European Wind Energy Association Conference* (Paris: European Wind Energy Association).
[10] Veers PS 1988 Three dimensional wind simulation *SAND88 – 0152* (Albuquerque: Sandia National Laboratories).
[11] Larsen X G *et al* 2013 Spectral structure of mesoscale winds over the water *Q. J. R. Meteorol. Soc*. 139: 685–700, April 2013.
[12] IEC 2004 Wind turbine generator systems - Part 1: Safety requirements*, IEC 1400-1 edition 3*.
[13] Ainslie J F 1988 Calculating the flowfield in the wake of wind turbines *J. Wind Engineering and Industrial Aerodynamics* **27**.
[14] Quarton D C & Ainslie J F 1990 Turbulence in Wind Turbine Wakes *Wind Engineering* **14**-1.
[15] Hassan U 1993 A wind tunnel investigation of the wake structure within small wind turbine farms *ETSU WN 5113*.
[16] Larsen G *et al* 2008 Wake meandering – a pragmatic approach *Wind Energy* **11**: 377-395.
[17] De Mare M 2015 Wake dynamics in offshore wind farms *PhD-0048 (EN)* (Copenhagen: DTU Wind Energy).
[18] Gebraad P M O 2014 Data-driven wind plant control *PhD Thesis* (T U Delft).
[19] Gunn K *et al* 2016 Limitations to the validity of single wake superposition in wind farm yield assessment *WindEurope Summit 2016*, *J. Phys Conference Series 749* (IOP).
[20] Bossanyi E *et al* 2013 Long-term simulations for optimising yaw control and start-stop strategies *Proc. European Wind Energy Conference* (Vienna: EWEA).
[21] Grunnet J *et al* 2010 Aeolus toolbox for dynamics wind farm model, simulation and control *Proc. European Wind Energy Conference* (Warsaw: EWEA).
[22] Poushpas S *et al* 2014 Wind farm control through dynamic coordination of wind turbines reference power, *Proc. 1st Int. Conf. on Renewable Energies Offshore* (Lisbon: Taylor & Francis).

Acknowledgments

 This project has received funding from the European Union's Horizon 2020 research and innovation programme under grant agreement nos. 727477 (CL-Windcon) and 727680 (TotalControl).